Microfluid Nanofluid (2011) 11:353–358
DOI 10.1007/s10404-011-0800-y

SHORT COMMUNICATION

Ultrafast measurement of transient electroosmotic flow in microfluidics

Cuifang Kuang · Rui Qiao · Guiren Wang

Received: 30 December 2010 / Accepted: 28 March 2011 / Published online: 21 April 2011

Abstract We present a non-intrusive molecular dye based method, i.e., laser-induced fluorescence photobleaching anemometer (LIFPA), to significantly increase temporal resolution (TR) for velocity measurement of fast transient electrokinetic flows. To our knowledge, the TR has been for the first time achieved to 5–10 μs, about 100 times better than that published from state-of-the-art micro particle image velocimetry (μPIV), which is currently the most widely used velocimetry in the microfluidics community. The new method provides us with new opportunities to study experimentally the fundamental phenomena of unsteady electrokinetics (EK) and to validate relevant theoretical models. One application of the new method is demonstrated by measuring the rise time of DC electroosmotic flows (EOFs) in a microcapillary of 10 μm in diameter.

Keywords Laser-induced fluorescence photobleaching anemometer · LIFPA · DC electroosmotic flow · Rise time · Transient electrokinetic flow

C. Kuang · G. Wang (✉)
Biomedical Engineering Program & Department of Mechanical Engineering, University of South Carolina, Columbia, SC 29208, USA
e-mail: guirenwang@sc.edu

C. Kuang
State Key Lab of Modern Optical Instrumentation, Zhejiang University, Hangzhou 310027, China

R. Qiao
Department of Mechanical Engineering, Clemson University, Clemson, SC 29634-0921, USA

1 Introduction

Electrokinetics (EK) is widely used for sample actuation, particle manipulation, and analyte separation in microfluidics for lab-on-a-chip applications. Although electrokinetic flows are often steady, alternative current (AC) EK and transient EK phenomena have recently received significant attention (Chang and Wang 2008; Kang et al. 2002; Yan et al. 2006) given the many advantages they offer over DC EK. In prior works, it was found that transient flow depends on the transverse size of the channel and may provide some unique property. For instance, pulsed DC electric fields can enhance separation based on electrophoresis (Frumin et al. 2001; Lin et al. 2008; Pel et al. 2009) and the fidelity of the pulse, which is related to the rise time of electroosmotic flow (EOF), can affect the separation efficiency (Heiger et al. 1992). AC EK is an intrinsically unsteady process, so are the initial phase of EOF and sample injection, etc. For example, in the initial phase of EOF, several dynamic processes occur including propagation of the electric field, capacitive charging of the double layer, resistive heating of the electrolyte and subsequent development of thermal gradients in both electrolyte and substrate (Dose and Guiochon 1993). The rise time (t_r) of this transient EOF is estimated to be on the order of 10^{-9}–10^{-5}s in microchannels depending on the position in the transverse direction (Söderman and Jönsson 1996). Furthermore, in AC EK devices such as pumps and mixers (Bazant and Ben 2006), fluid response often occurs at a time scale of $\sim 10^{-5}$–10^{-4} s (Bazant et al. 2009). To help understand these transient flows, measurement of the unsteady flow velocity with high temporal resolution (TR) is required.

Among the methods that have been used to measure fluid velocity in microfluidics, micro particle image velocimetry (μPIV) is most widely used. However, to our

knowledge, the published highest TR with μPIV for microfluidics system is on the order of ~500 μs (Shinohara et al. 2004, Yan et al. 2006), which is too slow to measure the aforementioned transient flows in microfluidics. We also note that the temporal resolution of PIV is different from the inverse of the frame rate per second of a camera. There are some other methods, such as nuclear magnetic resonance (Hunter and Callaghan 2007), hot wire anemometer (HWA) (Bruun et al. 1989), caged-fluorescence visualization (Ross et al. 2001), holographic optical velocimetry (Di Leonardo et al. 2006), laser Doppler velocimetry (LDV) (Pak et al. 1992), molecular tagging velocimetry (MTV), (Hu and Koochesfahani 2006; Roetmann et al. 2008) particle tracking velocimetry (PTV) (Wang et al. 2006), PIV (Adrian 2005; Devasenathipathy et al. 2002; Santiago et al. 1998) and invasive atomic force microscopic velocimetry (Piorek et al. 2006). All these methods have limited TR for microfluidics. For example, though the HWA allows for a dynamic response up to several hundreds of kHz in conventional aerodynamics (Mischler et al. 1995), its application in microfluidics can be difficult due to its intrusive nature, e.g., it can significantly disturb fluid flows and electric field in EK when used for measurement at different transverse positions in microchannels.

Molecular tracer based fluorescence recovery after photobleaching (FRAP) has been used to measure molecular diffusion for a long time (White and Stelzer 1999). Flamion et al. (1991) have improved this method to measure convection velocity as well, but this recovery method still has to "wait" for the fluorescence recovery, and thus, its TR is on the order of milliseconds. In order to achieve higher TR, "waiting" should be avoided for the fluorescence recovery.

Laser-induced fluorescence photobleaching anemometer (LIFPA) (Kuang and Wang 2009; Sugarman and Prud'homme 1987) presented here is different from the aforementioned photobleaching (PB)-based methods for measuring flow velocity. LIFPA has shown high potential to measure transient flows with ultrahigh temporal and spatial resolution simultaneously (Kuang and Wang 2010; Kuang et al. 2009a, b). The spatial resolution has recently been achieved to ~70 nm when stimulated emission depletion (STED) is employed to overcome the classical Abbe's diffraction limit (Kuang and Wang 2010). In this molecular tracer based method, PB is leveraged and a precalibrated relationship between flow velocity and fluorescence intensity is established. Therefore, no "waiting" for the fluorescence recovery is required, and thus, transient flows can be rapidly measured, if the PB is sufficiently fast. However, this method has so far only achieved a TR with 100 μs (Kuang et al. 2009a), which is still slower than required for measurement in many transient EK flows. In this article, we present a significantly increased TR of 5–10 μs in LIFPA by (1) applying a laser with a short wavelength and (2) increasing the laser power.

2 Principle of LIFPA

Laser-induced fluorescence photobleaching anemometer is based on a simplified model illustrating the relationship between fluorescence intensity I_f and fluid velocity u for a given dye concentration due to LIFP (Wang and Fiedler 2000). In this model, when the bleaching time t is approximated as the dye residence time within the laser beam of the detection point, I_f increases with u, i.e.

$$I_f = I_{f0}e^{-t/\tau} = I_{f0}e^{-d_f/(u\tau)} \quad (1)$$

where I_{f0} represents I_f at $t = 0$, τ denotes photobleaching time constant, e.g., half decay time, d_f, is beam width. This is a simplified model of the LIFPA, and more detailed models are also available (Crimaldi 1997; Rička 1987). In reality, τ as a system parameter depends on laser wavelength and intensity at the detection point, type of dye and buffer, etc. For a given bleaching time, the smaller τ, the lower I_f. Thus, lower τ causes faster bleaching, and higher dI_f/dt, i.e., higher temporal resolution. τ decreases with reduced laser wavelength and increased laser intensity. The parameter τ can be determined through experiment.

Note at the detection point, molecular diffusion will cause fluorescence recovery of the bleached dye molecules. However, LIFPA here does not measure the recovery, as some of other photobleaching-based velociometers do. In LIFPA, a calibration curve between u and I_f is measured first, if quantitative measurement of u is required. In this case, the recovery effect has already been included in the calibration relation. This is the main reason why LIFPA has high temporal resolution.

3 Experimental methods

In order to validate the ultrafast TR of LIFPA, the rise time t_r of DC EOFs is measured, since (1) this is one of the most basic transient electrokinetic flows and a very fast dynamic process (Söderman and Jönsson 1996); (2) the flow response understood here can help understand the AC EOF during each period of the AC signal. Theoretical works (Dose and Guiochon 1993; Söderman and Jönsson 1996) show that t_r decreases as the inner diameter (ID) of a capillary shrinks. The closer to the capillary wall, the faster the fluid velocity approaches the steady state (Söderman and Jönsson 1996). To study the DC rise time, previously the transverse size of the channel used was larger than 1 mm due to limited temporal resolution (Manz et al. 1995;

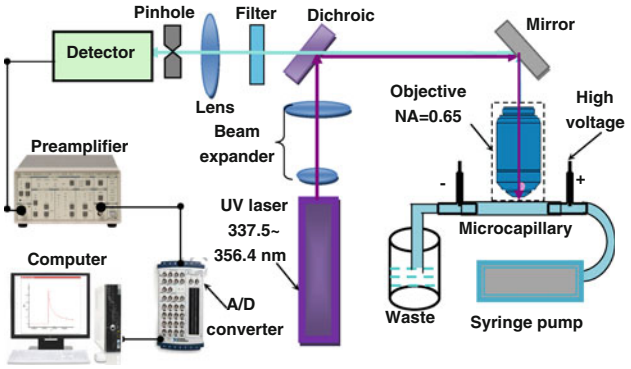

Fig. 1 Schematic of the experimental setup

Wu et al. 1995). In microfluidics, the transverse size is often on the order of 10 μm. To demonstrate the high spatial resolution of the LIFPA, here, we measure the t_r in a microcapillary with ID of 10 μm.

We now describe the experimental setup schematically shown in Fig. 1. A fused silica microcapillary (from Polymicro Technology) was used. It was placed on a precise 3D translation stage. A syringe pump drove a syringe containing fluorescence dye solution to deliver fluids to the microcapillary. Two Tee connections were used to connect tubing and platinum electrodes, respectively. The distance between the ends of the two platinum electrodes was about 50 mm and the detection position was 25 mm from the electrode at the entrance of the capillary. A high voltage power supply Keithley 248 (Keithley Instruments Inc., OH) was used to provide 0–5 kV DC signal for generating the EOF. A fast relay was built in a circuit loop to provide rapid switching of high voltages to the microcapillary. The relay was driven by a function generator, i.e. AFG3102 (Tektronix Corp. TX). The voltage of the power supply can be switched from zero to 2000 V in less than 0.3 μs, which is sufficiently short to satisfy the requirement of the experiments and has almost no effect on the measurement of t_r (Kuang et al. 2009a).

According to prior publications (Flamion et al. 1991; Wang and Fiedler 2000a, b), shot noise can be reduced by raising the dye concentration. A neutral dye (Coumarin 102) was diluted with pure methanol to a concentration of 200 μM for the experiments. The neutral dye as tracer can avoid error caused by electrophoresis, when EOF is measured. Coumarin 102 is selected, since this dye has a high quantum yield of photobleaching (number of photobleached molecules/total number of absorbed photons), i.e., 4.3×10^{-4} (Eggeling et al. 1998). Methanol is used as a working fluid since it is a good solvent for Coumarin 102. The Debye length (λ_D) of the solution is estimated to be on the order of 100 nm (Kim et al. 2008).

A Saber R series krypton laser from Coherent Inc, which was set to multi-UV wavelength mode, i.e., 337.5–356.4 nm, was used to excite the dye solution. The multi-UV can provide higher laser power from this laser to enhance photobleaching quantum efficiency. The laser power was set to about 250 mW (after the objective lens). After a beam expander the laser beam was reflected to a 40× and 0.65 NA objective by the dichroic mirror to excite the dye in the test section of the microcapillary. The focused laser beam diameter at the detection point is estimated to be about 350 nm. To avoid heat influence, a low pressure driven steady flow was added before measuring the EOF. The pressure driven flow and EOF can greatly remove potential heat generated by the laser beam. Fluorescence signal from the capillary was collected by the same objective, through the dichroic mirror and an optical bandpass filter, and focused to a detector, i.e., a photomultiplier tube (PMT) by a convex lens ($f = 100$ mm). Fluorescence signal was detected confocally through a pinhole, whose diameter was 10 μm in front of the PMT. The signal from the detector was amplified by a preamplifier SR570 (Stanford Research System, CA) and then acquired by an A/D converter USB-6259 (National Instruments, TX). The data sampling rate of the A/D converter and the bandwidth of the preamplifier were set to

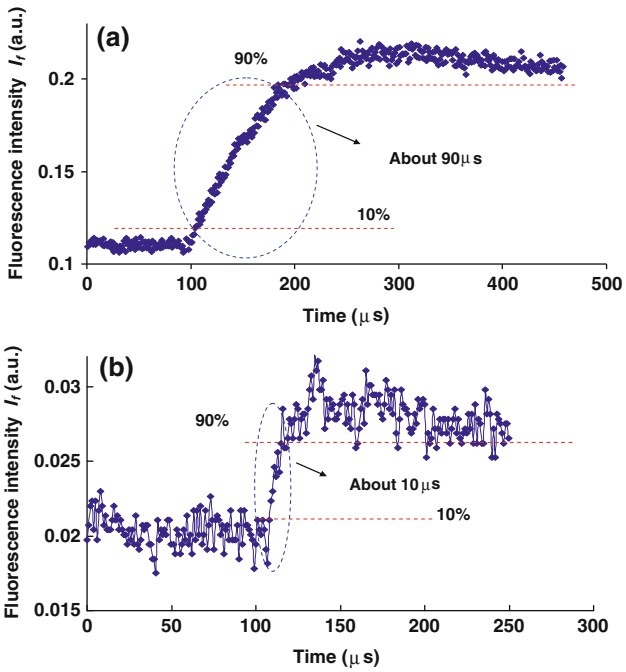

Fig. 2 Experimental results demonstrating ultrahigh TR of the LIFPA technique. **a** The time evolution of fluorescence intensity at detention point on the microcapillary axis. **b** The time evolution of fluorescence intensity at detection point 1 μm from the microcapillary wall. The detection points are 25 mm from the entrance of the capillary. Both panels show the dynamic process of EOF when a 2 kV voltage was switched on within 0.27 μs. Neutral dye was used to track the transient variation of the EOF velocity and to minimize systematic errors due to the electrophoresis effect

1 MHz for the data acquisition. The response of the PMT is 27 ns. Thus, the rise time of the measuring system should be in the order of 1 μs limited by the preamplifier.

4 Results and discussion

The ultrahigh TR of LIFPA is shown in Fig. 2 for an EOF with an applied voltage of 2000 V. Detection points in Fig. 2a and b are on the axis and at 1 μm from the wall of the capillary, respectively. Both points are out of the electric double layer (EDL). The relative location was determined for the detection point with respect to the capillary (at the center line or 1 μm from the wall) through a precise translation stage with a spatial resolution of 1–10 nm. The transient variation of EOF velocity u was recorded at the detection point, when a fast step of voltage increase was supplied to drive the flow in the microcapillary. In LIFPA, the higher the flow velocity, the larger the fluorescence signal (Kuang et al. 2009b; Wang 2005). As shown in Fig. 2a, it takes about 90 μs for the EOF to rise from 10 to 90% of its maximum steady state value on the capillary axis. When the measurement point was near the wall, t_r decreased to about 10 μs in Fig. 2b). Here, although the fluorescence signal was not converted to velocity by a pre-calibration relation, it does directly reflect the variation of transient velocity at the detection point—the focus of this work, since the fluorescence signal increases with the increased flow velocity, when other parameters are given (Kuang et al. 2009b; Wang 2005). Quantitative determination of the velocity can be obtained through a calibration and is documented in our prior publications (Kuang et al. 2009b; Wang 2005).

Figure 2b shows the transient process with time step of 1 μs during a 10 μs period. During the rise of EOF, the fluorescence intensity in principle should only increase, but it does decrease as well. We expect that this is because of shot noise. Considering the high frequency shot noise, the TR in the current system is evaluated to be 5–10 μs from Fig. 2b, if the TR is here defined as the duration, during which, the change in signal can be distinguished.

To explore LIFPA's potential impact on research in transient electrokinetic flow, we discuss two cases below. Firstly, note that LIFPA is so fast that we can even measure the overshot of the EOF velocity at the initial stage (cf. Fig. 2). To our knowledge, this is the first time such a phenomenon is observed in single microchannel, and it has not been reported in previous theoretical studies of transient EOFs (Dose and Guiochon 1993, Söderman and Jönsson 1996).

Secondly, we studied the dependence of EOF rise time on the microcapillary ID. The EOF rise time is an important parameter for AC EK and capillary electrophoresis in microfluidics. The rise time was first measured and then compared with theoretical prediction based on the work from Söderman and Jönsson (1996). Note in applying the theory, the following assumptions are used (Dose and Guiochon 1993): (1) The temperature is assumed uniform over the entire sample, because the timescale of relaxation of the solution velocity is much shorter than heating timescales at the lumen wall (Dose and Guiochon 1993). (2) The magnetic field produced by moving charge is neglected. (3) The flow is laminar and incompressible. (4) It is assumed that there is no counter-flow of liquids due to pressure gradient. (5) All the boundary surface charge density is assumed to be uniform. (6) The initial time is ignored when the velocity within a couple of Debye lengths outside the charged surface, reaches its maximum velocity.

Figure 3 shows the measured relationship between the ID and t_r at the axis of the capillary. In general, the measured values are higher than the theoretical predictions. It can be seen that, in the widest capillary, the experimental results agree well with the theoretical predication, which is consistent with that reported in millimeter-scale capillaries (Manz et al. 1995; Wu et al. 1995). The measured t_r in the 75 μm microcapillary is about 37% higher than the theoretical prediction. However, it is found that the relative deviation between the experimental measurement and the theoretical prediction increases rapidly with the decrease of the ID. For instance, as ID approaches to 10 μm, the measured t_r is about 400% higher than the predicted one. Since the TR of the system is much better than the measured 90 μs, the reason of the deviation should not be because of poor TR. At present, the above observation is not well-understood yet.

We postulate that one of the main reasons of the aforementioned difference may be related to a RC circuit effect of the microcapillary system. A microcapillary

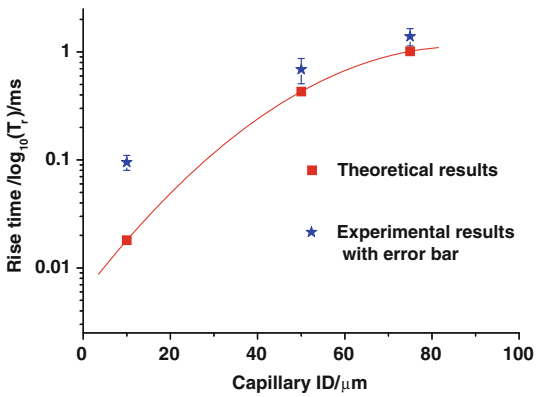

Fig. 3 Comparison of the measured t_r on the axis in microcapillaries having ID of 10, 50, and 75 μm, respectively, with theoretical prediction. (*Note*: the experimental data for 50 and 75 μm ID are obtained from another work (Kuang et al. 2009a) in order to compare the influence of ID on the rise time t_r of EOF)

integrated with electrodes can be modeled as an equivalent RC circuit. Specifically, the bulk electrolyte behaves as an electric resistor, and the EDLs at the interface between the bulk electrolyte and electrode act as capacitors as the electric field is switched on suddenly. The charging time constant τ_c of the capacitor is proportional to RC, i.e., the product of the electric resistance R of the medium and the capacitance C of the capacitor. The resistance R is inversely proportional to the square of the ID (Heiger et al. 1992), and the capacitance C can be approximated as (Kirby 2010)

$$C \sim \frac{\varepsilon A}{\lambda_D} \tag{2}$$

where ε is the dielectric permittivity, λ_D and A are the Debye length of the electrolyte and the area of the electrode in contact with the electrolyte, respectively. We note that Eq. 2 is valid strictly only at electrode potential much smaller than the thermal voltage, and more sophisticated models must be used under other conditions. However, for the present qualitative analysis, Eq. 2 is sufficient.

The charging time of the capacitor could affect the time required to establish the electric field inside the microcapillary system. However, most transient EOF theories have so far neglected the rise time of the electric field (t_{re}) itself in microcapillaries (Dose and Guiochon 1993; Söderman and Jönsson 1996). These theories are accurate in wide channels. In such channels, where the resistance is small, t_{re} is small and the rise of the electric field is much shorter than the rise time of EOF predicted by the theory, in which the electric field is switched on instantaneously (Söderman and Jönsson 1996). As such, neglecting the finite rise time of the electric field will incur at most small error in the rise time of the EOF. However, as the ID of a microcapillary is reduced, its resistance will increase rapidly but the total capacitance of the microcapillary system will remain the same as ε, λ_D, and A can be approximated as independent of ID. Consequently, the electric field rise time t_{re}, which is propositional to the product of the resistance and the capacitance, will increase sharply as ID is reduced, and may no longer be negligible compared to the rise time of the EOF generated by a suddenly imposed electric field. Consequently, the rise time of the EOF in these microcapillaries is larger than that predicted by the current theoretical models, and the discrepancy increases as the ID decreases. From the above discussion, it becomes clear that the dynamics of transient EOFs can be very complicated in narrow microchannels or in nanofluidic channels. Furthermore, the initial time may no longer be negligible when the velocity within a few Debye lengths outside the charged surface reaches its maximum velocity, since as the ID decreases, the ratio of this initial time to the entire rise time of EOF will increase. In order to fully understand and describe t_r, when the transverse dimension is sufficiently small, the theory should address other factors, such as the finite time required for the establishment of the electric field. In addition, assumptions (5) and (6) in the current models may need to be revised as well. Developing such a theory is out of the scope of the this study, but will be pursued in the future.

5 Conclusions

LIFPA with ultrahigh TR has been introduced for measuring fast transient EOFs. The method, for the first time, can measure the rise time of DC EOF in a microcapillary of 10 μm ID with a TR of 5–10 μs. The method could provide a new opportunity for measurement of velocity in transient electrokinetic flows in microfluidics and even in nanofluidics, when a pre-calibrated relationship between the velocity and fluorescence intensity is established.

Acknowledgments G.W. and R.Q. gratefully acknowledge support from NSF under grant No. CAREER CBET-0954977 and CBET-0756496, respectively. The work has also been partially supported by an NSF RII grant EPS-0447660. The authors are grateful to colleagues Wei Zhao and Muhammad Yakut Ali for helpful discussions.

References

Adrian RJ (2005) Twenty years of particle image velocimetry. Exp Fluids 39:159–169

Bazant MZ, Ben Y (2006) Theoretical prediction of fast 3D AC electro-osmotic pumps. Lab Chip 6:1455–1461

Bazant MZ, Kilicb MS, Storey BD, Ajdarid A (2009) Towards an understanding of nonlinear electrokinetics at large applied voltages in concentrated solutions. Adv Colloid Interface Sci 152:48–88

Bruun HH, Farrar B, Watson I (1989) A swinging arm calibration method for low velocity hot-wire probe calibration. Exp Fluids 7:400–404

Chang CC, Wang CY (2008) Starting electroosmotic flow in an annulus and in a rectangular channel. Electrophoresis 29:2970–2979

Crimaldi JP (1997) The effect of photobleaching and velocity fluctuations on single-point LIF measurements. Exp Fluids 23:325–330

Devasenathipathy S, Santiago JG, Takehara K (2002) Particle tracking techniques for electrokinetic microchannel flows. Anal Chem 74:3704–3713. doi:10.1021/ac011243s

Di Leonardo R, Leach J, Mushfique H, Cooper JM, Ruocco G, Padgett MJ (2006) Multipoint holographic optical velocimetry in microfluidic systems. Phys Rev Lett 96:134502–134504

Dose EV, Guiochon G (1993) Timescales of transient processes in capillary electrophoresis. J Chromatogr A 652:263–275

Eggeling C, Widengren J, RR C, Seidel AM (1998) Photobleaching of fluorescent dyes under conditions used for single-molecule detection: evidence of two-step photolysis. Anal Chem 70:2651–2659

Flamion B, Bungay PM, Gibson CC, Spring KR (1991) Flow rate measurements in isolated perfused kidney tubules by fluorescence photobleaching recovery. Biophys J 60:1229–1242

Frumin LL, Peltek SE, Zilberstein GV (2001) Nonlinear electrophoresis and focusing of macromolecules. J Biochem Biophys Methods 48:269–282

Heiger DN, Carson SM, Cohen AS, Karger BL (1992) Wave form fidelity in pulsed-field capillary electrophoresis. Anal Chem 64:192–199. doi:10.1021/ac00026a019

Hu H, Koochesfahani MM (2006) Molecular tagging velocimetry and thermometry and its application to the wake of a heated circular cylinder. Meas Sci Technol 17:1269–1281

Hunter MW, Callaghan PT (2007) NMR measurement of nonlocal dispersion in complex flows. Phys Rev Lett 99:210602–210604

Kang Y, Yang C, Huang X (2002) Dynamic aspects of electroosmotic flow in a cylindrical microcapillary. Int J Eng Sci 40:2203–2221

Kim D, Posner JD, Santiago JG (2008) High flow rate per power electroosmotic pumping using low ion density solvents. Sens Actuators A 141:201–212

Kirby B (2010) Micro- and nanoscale fluid mechanics—transport in microfluidic devices. Cambridge University Press, Cambridge

Kuang C, Wang G (2010) A far-field nanoscopic velocimeter for nanofluidics. Lab Chip 10:240–245

Kuang C, Yang F, Zhao W, Wang G (2009a) Study of the rise time of electroosmotic flow within a microcapillary. Anal Chem 81:6590–6595

Kuang C, Zhao W, Yang F, Wang G (2009b) Measuring flow velocity distribution in microchannels using molecular tracers. Microfluid Nanofluid 7:509–517

Lin C-H, Wang J-H, Fu L-M (2008) Improving the separation efficiency of DNA biosamples in capillary electrophoresis microchips using high-voltage pulsed DC electric fields. Microfluid Nanofluid 5:403–410

Manz B, Stilbs P, Joensson B, Söderman O, Callaghan PT (1995) NMR imaging of the time evolution of electroosmotic flow in a capillary. J Phys Chem 99:11297–11301. doi:10.1021/j100029a001

Mischler M, Fan-Gang T, Ulmanella U, Chih-Ming H, Fukang J, Yu-Chong T (1995) A micro silicon hot-wire anemometer. In: TENCON '95, IEEE region 10 international conference on microelectronics and VLSI

Pak HK, Goldburg WI, Sirivat A (1992) Measuring the probability distribution of the relative velocities in grid-generated turbulence. Phys Rev Lett 68:938

Pel J, Broemeling D, Mai L, Poon H-L, Tropini G, Warren RL, Holt RA, Marziali A (2009) Nonlinear electrophoretic response yields a unique parameter for separation of biomolecules. Proc Natl Acad Sci 106:14796–14801

Piorek B, Mechler A, Lal R, Freudenthal P, Meinhart C, Banerjee S (2006) Nanoscale resolution microchannel flow velocimetry by atomic force microscopy. Appl Phys Lett 89:153123

Rička J (1987) Photobleaching velocimetry. Exp Fluids 5:381–384

Roetmann K, Schmunk W, Garbe C, Beushausen V (2008) Microflow analysis by molecular tagging velocimetry and planar Raman-scattering. Exp Fluids 44:419–430

Ross D, Johnson TJ, Locascio LE (2001) Imaging of electroosmotic flow in plastic microchannels. Anal Chem 73:2509–2515. doi:10.1021/ac001509f

Santiago JG, Wereley ST, Meinhart CD, Beebe DJ, Adrian RJ (1998) A particle image velocimetry system for microfluidics. Exp Fluids 25:316–319

Shinohara K, Sugii Y, Aota A, Hibara A, Tokeshi M, Kitamori T, Okamoto K (2004) High-speed micro-PIV measurements of transient flow in microfluidic devices. Meas Sci Technol 15:1965–1970

Söderman O, Jönsson B (1996) Electro-osmosis: velocity profiles in different geometries with both temporal and spatial resolution. J Chem Phys 105:10300–10311

Sugarman J, Prud'homme R (1987) Effect of photobleaching on the output of an on-column laser fluorescence detector. Ind Eng Chem Res 26:1449–1454

Wang GR (2005) Laser induced fluorescence photobleaching anemometer for microfluidic devices. Lab Chip 5:450–456

Wang GR, Fiedler HE (2000a) On high spatial resolution scalar measurement with LIF Part 2: the noise characteristic. Exp Fluids 29:265–274

Wang GR, Fiedler HE (2000b) On high spatial resolution scalar measurement with LIF. Part 1: photobleaching and thermal blooming. Exp Fluids 29:257–264

Wang S-Q, Ravindranath S, Boukany P, Olechnowicz M, Quirk RP, Halasa A, Mays J (2006) Nonquiescent relaxation in entangled polymer liquids after step shear. Phys Rev Lett 97:187801–187804

White J, Stelzer E (1999) Photobleaching GFP reveals protein dynamics inside live cells. Trends Cell Biol 9:61–65

Wu DH, Chen A, Johnson CS (1995) Flow imaging by means of 1D pulsed-field-gradient NMR with application to electroosmotic flow. J Magn Reson Ser A 115:123–126

Yan D, Nguyen N-T, Yang C, Huang X (2006) Visualizing the transient electroosmotic flow and measuring the zeta potential of microchannels with a micro-PIV technique. J Chem Phys 124:021103–021104